

## Prediction and Optimization of the Effects of Combining Ultrasonic Waves and Solvent on the Viscosity of Residue Fuel Oil by ANN and ANFIS

A. Mohammadi Doust<sup>a</sup>, M. Rahimi<sup>a</sup> and M. Feyzi<sup>b,\*</sup>

<sup>a</sup>Department of Chemical Engineering, Faculty of Engineering, Razi University, Kermanshah, Iran

<sup>b</sup>Faculty of Chemistry, Razi University, P. O. Box: +98-67149, Kermanshah, Iran

(Received 8 January 2016, Accepted 16 March 2016)

In the present work, the influences of temperature, solvent concentration and ultrasonic irradiation time were numerically analyzed on viscosity reduction of residue fuel oil (RFO). Ultrasonic irradiation was applied at power of 280 W and low frequency of 24 kHz. The main feature of this research is prediction and optimization of the kinematic viscosity data. The measured results of eighty-four samples, including 336 data points, were developed by artificial neural network (ANN) and adaptive neuro-fuzzy inference system (ANFIS). The ANN predictions were also compared with the ANFIS approach by means of various descriptive statistical indicators, including absolute average deviation (AAD), average relative deviation (ARD) and coefficient of correlation ( $R^2$ ). The AAD and  $R^2$  of the developed ANN model for kinematic viscosity prediction of overall set were 0.0107 and 0.99384, respectively. On the other hand, for ANFIS approach, the AAD of 0.02112 and  $R^2$  of 0.99279 were attained. Although accuracy and precision of the ANN model were more than the ANFIS approach, it has been illustrated that the proposed ANN and ANFIS models have a superior performance with acceptable errors on the RFO kinematic viscosity estimation. Findings of this research clearly revealed that the neural network and neuro-fuzzy approaches could be successfully employed for prediction and optimization of kinematic viscosity of RFO and high viscosity materials in oil processes.

**Keywords:** Residue fuel oil, Kinematic viscosity, Ultrasonic irradiation, Artificial Neural Network, Adaptive Neuro-Fuzzy Inference System

### INTRODUCTION

Oil fractions play important roles in human life. Residue fuel oil (RFO) as one of these fractions is extracted from bottom of atmospheric distillation column. Original oil and the subsequent processing are factors which can determine their compositions. Therefore, process type of crude oil refining is effective on different properties of RFOs. The complexity of residue fractions stems from the mass participation of simple groups combined to form complex molecules and countless isomers. Viscosity, boiling point, and carbon chain length are key factors taken account to classify the RFOs. Kinematic viscosity is the most significant factor in fuel oil transportation [1-3]. It is

valuable to find some ways to handle RFO by decreasing its kinematic viscosity. Thermal cracking [4-6], chemical [3,7,8], electromagnetic heating [9], acoustical method [10,11] and so on, are several methods for RFO treatment. Finding a new method is necessary for easy and simple transportation of residue fuel oil with high kinematic viscosity. Recently, ultrasonic waves irradiation has obtained as a novel method. Different frequencies of waves cause to produce the cavitation bubbles. Ultrasound irradiation leads to temperature and pressure variations. These variations are the main factors in formation of microscopic bubbles which spread extremely and generate millions of shock waves. Collapse of these bubbles rise the temperature and pressure. Cavitation phenomenon is effective on flow rheology, because of increasing the mass and heat transfer rates [9-11]. Ultrasonic irradiation

\*Corresponding author. E-mail: [m.feyzi@razi.ac.ir](mailto:m.feyzi@razi.ac.ir)

technique for treatment of asphaltene deposition was introduced by Shedid [12]. In that work, effect of ultrasonic irradiation, solvent concentration and temperature on asphaltene behavior in the UAE crude oil was investigated. The results demonstrated that the ultrasonic irradiation reduces the size of asphaltene clusters. Gogate [13] presented a critical review about cavitation reactors for the intensification process of chemical processing applications. The author designed a pilot-scale sonochemical reactor and explained its operations. Hongfu *et al.* [14] applied steam stimulation process for composition changes of heavy oils. After reaction with steam, the viscosity of heavy oil was reduced by 28-42% and the amount of the saturated and aromatic hydrocarbons increased, while resin and asphaltene decreased. The major problem of this method was reduction of combustion quality by using steam. Bjorndalen and Islam [15] investigated the effects of microwave and ultrasonic irradiation on crude oil during production with a horizontal well. The components of crude oil such as asphaltenes and paraffin wax can precipitate in the horizontal section of the well causing a loss of productivity and profit. Therefore, microwave or ultrasonic irradiation for removing these precipitates was essential. Hong-Xing and Chun-Sheng [16] used catalyst and ultrasonic irradiation for aquathermolysis of heavy crude oil. The results of ultrasonic irradiation assisted catalytic aquathermolysis indicated that the viscosity of heavy crude oil was reduced by 86.2% with the 53.91% heavy crude oil recovery. Moreover, the average molecular weight of heavy crude oil decreased, the saturate and aromatic contents increased and the resin and asphaltene contents reduced. Wang *et al.* [17] investigated the ultrasonic sludge disintegration for improving the co-slurrying properties of municipal waste sludge and coal. In that study, sludge was pretreated by ultrasonic energy and then mixed with coal to prepare coal sludge slurry (CSS). After ultrasonic pretreatment, sludge flocs were scattered, and their particle size significantly reduced. Ultrasonic improved the slurry ability of sludge and enhanced sludge disposal scale to a high level. Saikia *et al.* [18] used ultrasonic energy for cleaning of high sulphur Indian coals in water and mixed alkali. The changes in morphology of the ultrasonicated coal samples are explained due to the cavitation phenomenon in the coal structure. The ultrasonic energy interpreted the

possible mechanism of coal cleaning in that work.

In recent years, prediction and optimization of the crude oil properties has been found significant attention in literature [19-22]. Among this wealth of investigative effort, little attention has been paid on residue fuel oils. Artificial Neural Network (ANN) and Adaptive Neuro-Fuzzy Inference System (ANFIS) as artificial intelligence methods play important role in the modeling, prediction and optimization of complex systems. Yetilmezsoy *et al.* [23] developed an adaptive neuro-fuzzy approach for modeling water-in-oil emulsion formation. Density, viscosity, asphaltene, saturate, aromatic and resin contents were analyzed as responsible factors. The results showed that subtractive clustering method of a first-order sugeno type was capable for assessment and estimation of emulsion stability. Many researchers carried out the adaptive neuro-fuzzy inference system and artificial neural networks as suitable methods for estimation and evaluation of the complex processes [24-29].

The specific aims of this work are prediction and optimization of the effects of combining ultrasonic waves and solvent on the kinematic viscosity of fuel oil. For doing so, the artificial neural network (ANN) and adaptive neuro-fuzzy inference system (ANFIS) were developed. Comparison between ANN and ANFIS approaches, evaluation of the performance functions and verification of the models with experimental data were also performed.

## EXPERIMENTAL

### Experimental Setup

A schematic view from experimental setup is shown in Fig. 1. In this work, a sample from high viscosity of RFO was prepared. A cylindrical beaker with a volume of 300 ml, containing 100 ml of RFO, was used as a container. The top of the beaker was closed, and surrounded by cooling water as a cold bath at  $16 \pm 1$  °C.

In this work, an ultrasonic probe (UP400s, Hielscher Co., Germany) was used for decreasing the kinematic viscosity of residue fuel oils (with constant frequency of 24 kHz and a power varied in the range of 0-400 W). A probe with a diameter of 20 mm and a height of 30 cm was employed in the experiments. According to the laboratory results and optimization procedure, cycle of 0.5, 70%

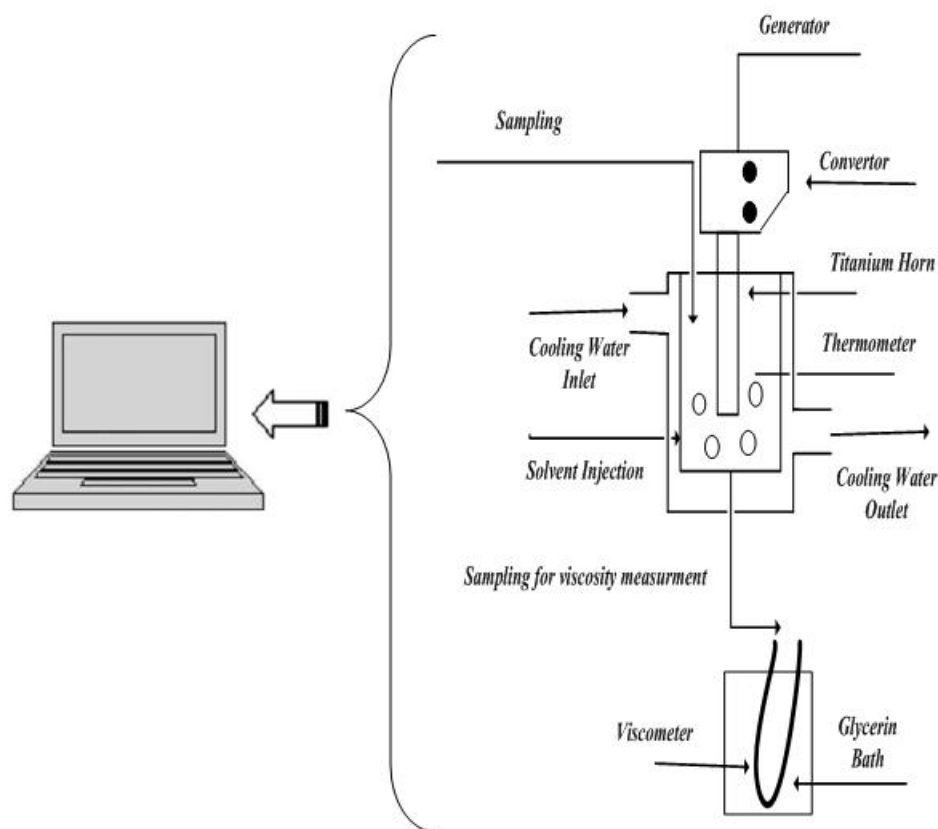


Fig. 1. Schematic of experimental setup.

amplitude and a power of 280 W, were selected. Eventually, for promotion the RFO viscosity reduction, various concentrations of solvent were injected into beaker.

According to ASTM D445 [30], a specific size of Cannon-Fenske Routine viscometer (Cole-Parmer Co., US) can be used for high viscosity measurements of RFO samples in a glycerin bath fixed at specified temperature  $\pm 1$  °C. After any change, API Gravity of fuel oil was also determined by API meter (Anton Paar Co., Austria) in experiments.

### Materials Preparation

The characteristics of RFO sample applied in this work are shown in Table 1. The sample was provided by Kermanshah oil refinery, Iran. In experiments, performance of acetonitrile (ACT-N) and toluene were compared. Finally, acetonitrile was selected because of its high

efficiency and less harm for human. The solvent was supplied from Merck Inc. with a high purity of 99%.

### Procedures

To investigate the influences of ultrasonic irradiation and solvent on decreasing the kinematic viscosity of RFO in various temperatures, according to Table 1, 100 ml of the RFO was placed in a 300 ml beaker and heated. The kinematic viscosity was measured at temperatures of 20, 30, 40 and 50 °C, respectively. Then, ultrasonic waves irradiated a new sample of the residue fuel oil for different time intervals of 5, 10 and 15 min. The kinematic viscosities of samples were determined at temperatures of 20, 30, 40 and 50 °C, respectively. Six different acetonitrile concentrations of 0.5, 1, 2, 3, 4 and 5% (v/v acetonitrile/RFO) were made using the same RFO, to study the effect of applied solvent. The solutions were heated and their

**Table 1.** The Characteristics of RFO Sample

Test	Results	ASTM	Ref.
Kinematic viscosity at 50 °C (cSt)	494	D 445	[30]
d <sup>20</sup> °C (g cm <sup>-3</sup> )	1.03	D 1298	[31]
Pour point (°C)	0	D 97	[32]
Ash	0.03%	D 482	[33]
Flash point (°C)	140	D 92	[34]

kinematic viscosities were measured at various temperatures. Furthermore, other solutions with the same concentrations were irradiated in the presence of ultrasonic waves for various time intervals. Finally, the kinematic viscosities of samples with combining ultrasonic waves and solvent were determined at various temperatures.

## ANALYSES OF EXPERIMENTAL DATA

### Artificial Neural Network (ANN)

In the present research, the MATLAB software was employed for the ANN modeling. The ANN includes some network types as Cascade-forward back propagation, Competitive, Elman back propagation, Feed-forward back propagation, generalized regression, Hopfield and so on. The feed-forward back propagation was used with a lower error compared with the other network types. This network type contains several algorithms such as: trainlm (Levenberg-Marquardt), traingda (Gradient Descent Back Propagation with Adaptive Learning Rate), trainbr (Bayesian Regularization), traincgb (Conjugate Gradient with Beale-Powell Restarts), trainrp (Random Propagation), trainscg (Scaled Conjugate Gradient), *etc.* Bayesian Regularization (trainbr) is modification of the Levenberg-Marquardt training algorithm to produce networks that generalize well [35]. It reduces the difficulty of determining the optimum network architecture. Finally, from among of these algorithms the trainbr was determined by optimization with high performance to estimate the kinematic viscosity of RFO, which will be explained in the subsequent sections.

In these networks, each neuron is connected to the

neurons of next layer. The data points are transferred by the connections. Each of these connections has a weight. The output of any connection would be based on the following equation:

$$y_j = F_t \left( \sum_{i=1}^n w_{ji} x_i + b_j \right) \quad (1)$$

In which,  $y_j$  is the output of  $j$ th neuron,  $w_{ji}$  is weight of  $j$ th neuron  $i$ th input,  $x_i$  is the independent variable,  $b_j$  is the  $j$ th neuron bias,  $n$  is number of input variables to  $j$ th neuron and  $F_t$  is the transfer function.

Many transfer functions are included in the neural networks. Three of the most commonly used functions are shown below:

$$\text{Hyperbolic tangent sigmoid (Tansig): } F_t(x) = \frac{e^x - e^{-x}}{e^x + e^{-x}} \quad (2)$$

$$\text{Purelin: } F_t(x) = x \quad (3)$$

$$\text{Logarithm sigmoid (Logsig): } F_t(x) = \frac{1}{1 + \exp(-x)} \quad (4)$$

In this study, the tansig and purelin transfer functions were considered for the hidden layer and output layer, respectively. In this training network, the weights and biases attempt to minimize the errors between output and target data. Hence, the calculation of the errors for different ANNs with the number of neurons of in input, output and hidden layers to peruse of network performance is very important.

In summary, the ANN model structure includes input

**Table 2.** The Range of Data Used in ANN Model

Variable	Min	Max
Temperature (°C)	20	50
Acetonitrile (vol.%)	0	5
Ultrasonic irradiation time (min)	0	15
Kinematic viscosity (cSt)	133	4940

layer, output layer and some hidden layers containing neurons. The neurons of each layer are connected by the special layers and an interconnected group was made by the weights and biases. Finally, a logical pattern between input and output parameters was produced. The number of input and output variables is determiner from the number of neurons in the input and output layers, while the number of neurons in the hidden layers was specified by trial-and-error and optimization which will be investigated in subsequent sections [35]. In this work, the ANN input data were temperature of sample (T), acetonitrile concentration (ACT-N) and ultrasonic irradiation time (UST). In addition, frequency, power, cycle and amplitude percent were constant at 24 kHz, 280 W, 0.5 and 70 based on the laboratory conditions, respectively. All input data points in ANN model randomly divided into three data sets consist of training (60%), validation (20%) and test (20%). The experimental data including eighty-four samples and 336 data points were collected from the laboratory measurements. Table 2 classifies the range of data points employed in this work for developing the ANN model.

### Adaptive Neuro-Fuzzy Inference System (ANFIS)

Artificial neural networks (ANNs) and fuzzy inference systems approaches have advantages and disadvantages through the modeling experimental data. For example, the ANNs do not present obvious relationships between input and target variables. There are also some problems of fuzzy inference systems which are complex and need to better understanding. Generally, artificial intelligence as a powerful tool plays an important role in the modeling of complex systems. Jang [36] developed the ANNs and fuzzy

systems to a new approach combining both methods. Adaptive neuro-fuzzy inference system (ANFIS) was proposed to overcome the shortcomings of ANNs and fuzzy inference systems. The ANFIS acts similar to ANNs in aspect of feed-forward back propagation type. The adaptive neuro-fuzzy inference system is made of two parts, preliminary and conclusion, which are joined to each other by fuzzy rules based on the network generation. The first-order sugeno inference system is used in fuzzy section. Output variables are produced by employing fuzzy rules to fuzzy sets of input variables [37-39]:

$$\text{Rule 1: If } (X_1 \text{ is } A_1) \text{ and } (X_2 \text{ is } B_1) \text{ then } f_1 = p_1 * X_1 + q_1 * X_2 + r_1 \quad (5)$$

$$\text{Rule 2: If } (X_1 \text{ is } A_2) \text{ and } (X_2 \text{ is } B_2) \text{ then } f_2 = p_2 * X_1 + q_2 * X_2 + r_2 \quad (6)$$

In which,  $p_1$ ,  $p_2$ ,  $q_1$  and  $q_2$  are linear parameters, and  $A_1$ ,  $A_2$ ,  $B_1$  and  $B_2$  are fuzzy sets.  $f_1$  and  $f_2$  are system's output. As seen in Fig. 2, the ANFIS configuration consists of five layers, fuzzy layer, product layer, normalized layer, defuzzy layer and total output layer.

In the fuzzy layer, each node  $i$  is an adaptive node with a distinct fuzzy membership function. The membership relationship between the output and input functions of this layer is as follows:

$$Q_i = \mu_{A_i}(X_1) \text{ or } \mu_{B_i}(X_2) \quad i = 1, 2 \quad (7)$$

Where,  $X_1$  and  $X_2$  are the inputs to node  $i$ ,  $A_i$  and  $B_i$  are fuzzy sets.  $Q_i$  is the output functions,  $\mu_{A_i}(X_1)$  or  $\mu_{B_i}(X_2)$

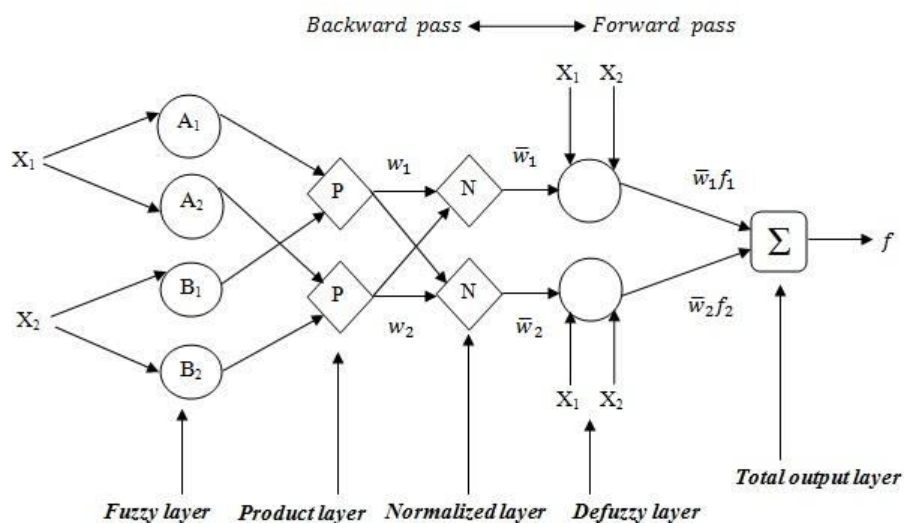


Fig. 2. The ANFIS configuration.

is membership function such as the Gaussian curve, generalized bell-shaped, *etc.* Following equations show some membership functions.

$$\mu_A(X) = \exp\left[-\frac{1}{2}\left(\frac{X - c_i}{\sigma_i}\right)^2\right] \quad (8)$$

$$\mu_A(X) = \frac{1}{1 + [(X - c_i / \sigma_i)^2] b_i} \quad (9)$$

In which  $\{\sigma_i, b_i, c_i\}$  is the parameter set.

The second layer, namely, product layer consists of two nodes which multiply the membership functions of inputs and produces the outputs.

$$w_i = \mu_{A_i}(X_1) * \mu_{B_i}(X_2) \quad i = 1,2 \quad (10)$$

Where,  $w_1$  and  $w_2$  are the weight functions of the next layer. The third layer is the normalized layer which  $i$ th node was normalized based on below equation.

$$\bar{w}_i = \frac{w_i}{w_1 + w_2} \quad i = 1,2 \quad (11)$$

Layer 4 is the defuzzy layer. Output of this layer is obtained

from normalized layer output multiplying the first-order of sugeno fuzzy rule as follows:

$$\bar{w}_i f_i = \bar{w}_i (p_i^* X_1 + q_i^* X_2 + r_i) \quad i = 1,2 \quad (12)$$

The fifth layer as the total output layer can be calculated as:

$$\text{Overall output} = \sum_i \bar{w}_i f_i = \frac{\sum_i w_i f_i}{\sum_i w_i} \quad (13)$$

In this study, the ANFIS toolbox of the MATLAB software was employed for modeling experimental data. Grid partition and subtractive clustering fuzzy inference systems were methods to generate the optimum fuzzy rules. The Grid method includes eight membership functions, trimf, trapmf, gbellmf, gaussmf, gauss2mf, pimgf, dsimgf, psimgf. The optimum rule numbers are attained based on the lowest error by human experts. The subtractive clustering approach supposes each data point is a potential cluster centre and determines a probability which each data point would define the cluster centre, based on the density of surrounding data points. The algorithm picks up the data point with the highest potential to be the first cluster centre and eliminates all data points in the nearby area of the first cluster center. In addition, it determines the next data cluster, its center

place and iterates on this process until all of the data points are within radii of a cluster center. There are four parameters of subtractive clustering algorithm, range of influence (ROI), squash factor (SF), accepted ratio (AR) and rejected ratio (RR) [40-42]. There are two training optimization methods in neural part of the system, hybrid and back propagation. In this research, two-third of data points as the training network and remaining data the testing network were considered (all of data points: 336). Subtractive clustering algorithm and optimization method of hybrid were also applied because of the best results.

## RESULTS AND DISCUSSION

In the experimental studies, the effects of temperature (T), solvent concentration (ACT-N%) and ultrasonic irradiation time (UST) on the kinematic viscosity of residue fuel oil (RFO) were investigated. The kinematic viscosity and API gravity as two important analyses were employed. In the first stage of experimental studies, sixteen samples of fuel oil were irradiated at different time intervals of 0, 5, 10 and 15 min and at temperatures of 20, 30, 40 and 50 °C. The results are shown in Fig. 3. As seen in this figure, maximum viscosity reduction is achieved at T = 50 °C. It is clear that the increase of temperature decreases fuel oil viscosity for all time intervals. In addition, by increasing of time to 5 min a significant reduction in the fuel oil viscosity was happened compared with that of the nonirradiated sample. Moreover, the enhancement of ultrasonic irradiation time to 10 and 15 min makes an increase in fuel oil viscosity. A significant increase was attained in viscosity for 15 min than ultrasonic irradiation time of 5 min. This can be explained by boiling effect due to generated heat and cavitation phenomenon assisting the evaporation of light components [9,12]. On the other hand, increase of fuel oil viscosity after 5 min can be attributed to a breakdown of large molecular of hydrocarbons such as asphaltene to more tiny cracked uniform particles in the fuel oil samples [9,12,43,44]. The boiling effect was started at 10 min and became more obvious at 15 min.

In general, the results show that the increase of solvent concentration decreases the fuel oil viscosity for all times of ultrasonic irradiation. This is because the increase of solvent concentrations increases solubility of some hydrocarbons

(saturates, asphaltenes, resins, aromatics) for each ultrasonic time. Figure 4. confirms above mentions. Finally, the maximum reduction of fuel oil viscosity (at 133 cSt) was measured at temperature of 50 °C, acetonitrile volumetric concentration of 5% and ultrasonic irradiation time of 5 min. In order to verify the experiments results, not only the kinematic viscosity but also the API Gravity index and FT-IR spectroscopy were analyzed. These tests were performed for evaluation of lightening and bond cracking of RFO. In the second analysis, the API (American Petroleum Institute) gravity index was measured. The API gravity is an index to evaluate the density of petroleum products. It depends on specific gravity at 60 °F. Specific gravity is relation of oil density per water density at reference temperature. The API gravity was defined based on the following equation [45]:

$$API\ Gravity = \frac{141.5}{Sp. Gr(60\ ^\circ F)} - 131.5 \quad (14)$$

Oil with API lower than ten is known as very heavy oil and between ten and twenty is heavy oil. Oil with API higher than twenty is placed in category of light oil.

In this work, the effects of ultrasonic irradiation time, solvent concentration and kinematic viscosity on the API gravity of RFO were also investigated. According to Fig. 5, the API increase is from zero to some times less than 5 min and after this time, it decreases based on the above reasons. On the other hand, as presented in Eq. (14), density of the sample declined for 5 min of ultrasonic irradiation. By increasing time, it gradually raised. Therefore, the optimum lightening of the sample was obtained at UST = 5 min and after this time, negative effect was observed. The API gravity and kinematic viscosity as two standard tests were employed in lightening and easy transportation of heavy oils. These tests were carried out based on the specific standards introduced in the previous sections. In summary, at temperature of 50 °C, with decreasing of viscosity, the API gravity increases because of cracking and lightening hydrocarbon bonds by ultrasonic irradiation power. Therefore, kinematic viscosity is in an inverse relation with the API gravity as illustrated in Fig. 6.

On the other hand, FT-IR spectroscopy was used to get detailed information about the structure through the modes of vibration. The results of FT-IR spectroscopy are

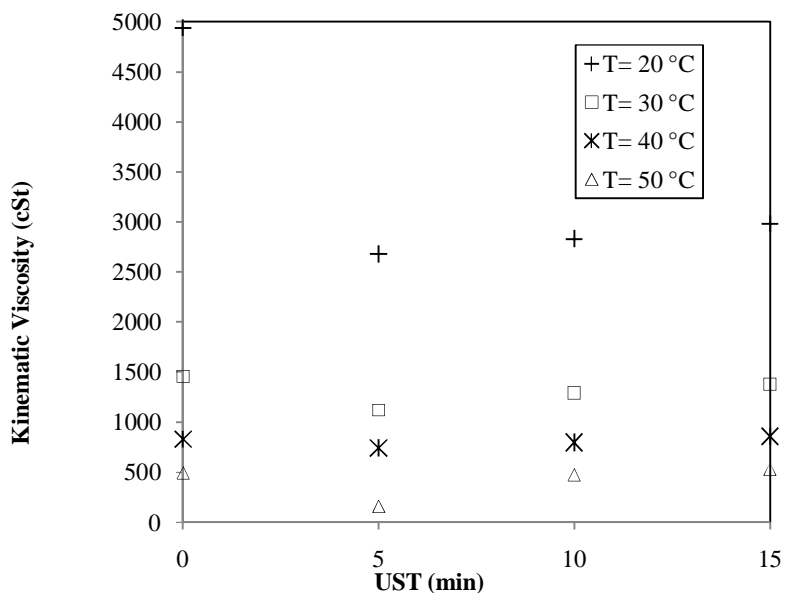


Fig. 3. Effect of ultrasonic irradiation on fuel oil viscosity at various temperatures.

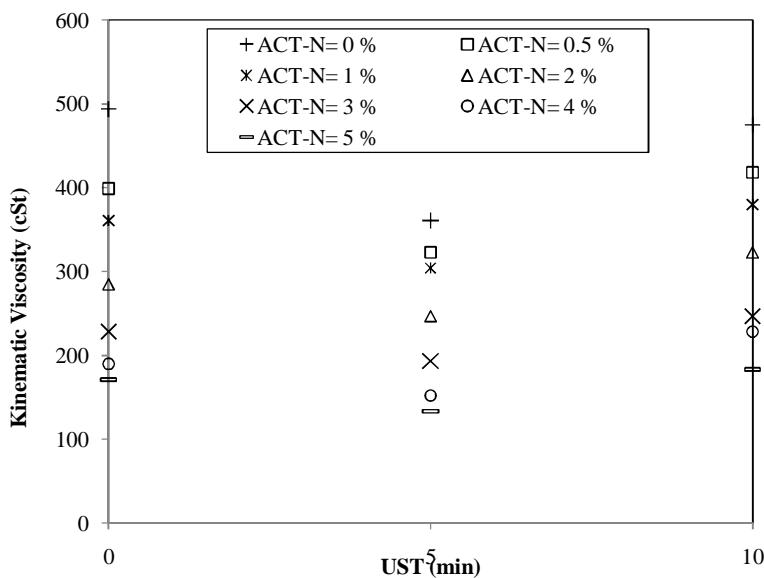
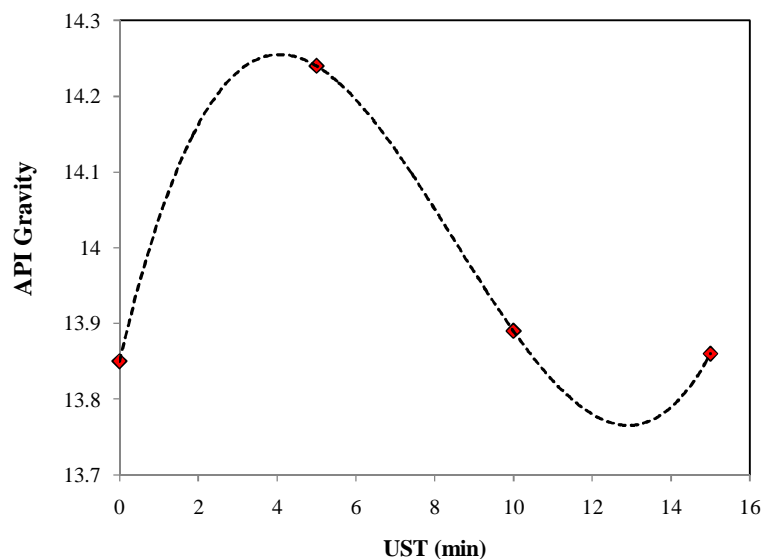


Fig. 4. Effects of combining ultrasonic radiation and acetonitrile concentrations on fuel oil viscosity (T = 50 °C).

displayed in Fig. 7. The bands at 2729 and 2932  $\text{cm}^{-1}$  correspond to stretching and bending modes of C-H linkage in the sample provided from Kermanshah Refinery. The spectrum of the two samples show some peaks at 1459  $\text{cm}^{-1}$  stretching modes of  $\text{CH}_2$ . The bands around 1375  $\text{cm}^{-1}$  correspond to  $\text{CH}_3$  fraction. The bands around 728-865  $\text{cm}^{-1}$

correspond to -C-C-C band in long hydrocarbon chain (aliphatic). These areas are fingerprinting area for evaluating of hydrocarbons chain length. These results showed that the intensity of signal bands around 728-865  $\text{cm}^{-1}$  decreased after ultrasonic irradiation. This suggested that the -C-C-C- bonding in long hydrocarbon chain was



**Fig. 5.** Effect of ultrasonic irradiation time on API gravity.

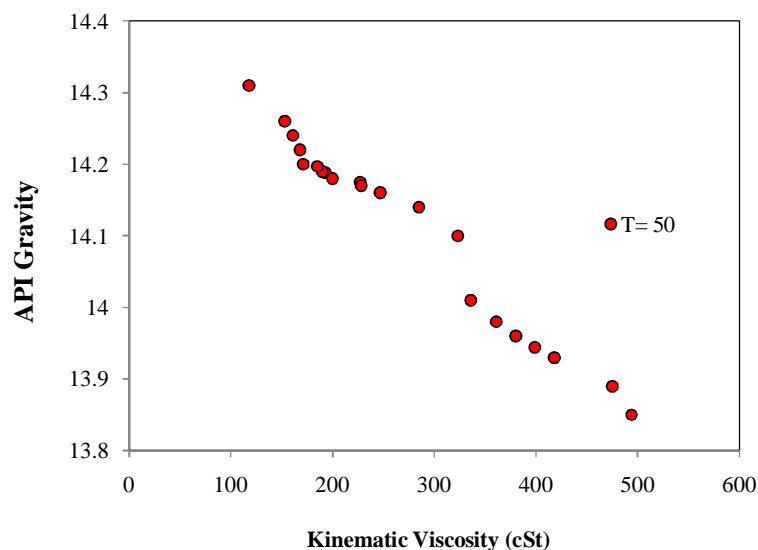


**Fig. 6.** Variations of kinematic viscosity and API gravity.

broken and short after ultrasonic irradiation.

### The ANN Modeling

In many studies, it has been endeavored to determine a good modeling for scrutinize and easily achievement of information. Analyzing and modeling data play an important role in accurate prediction of data. In this work,

the ANN model was developed to predict the kinematic viscosity of residue fuel oil. Temperature (T), volumetric concentration of solvent (ACT-N%), and ultrasonic irradiation time (UST) as input variables and kinematic viscosity ( $\nu$ ) as output variable were considered. Based on laboratory results, the ANN input variables were very effective on changes of kinematic viscosity selected for the

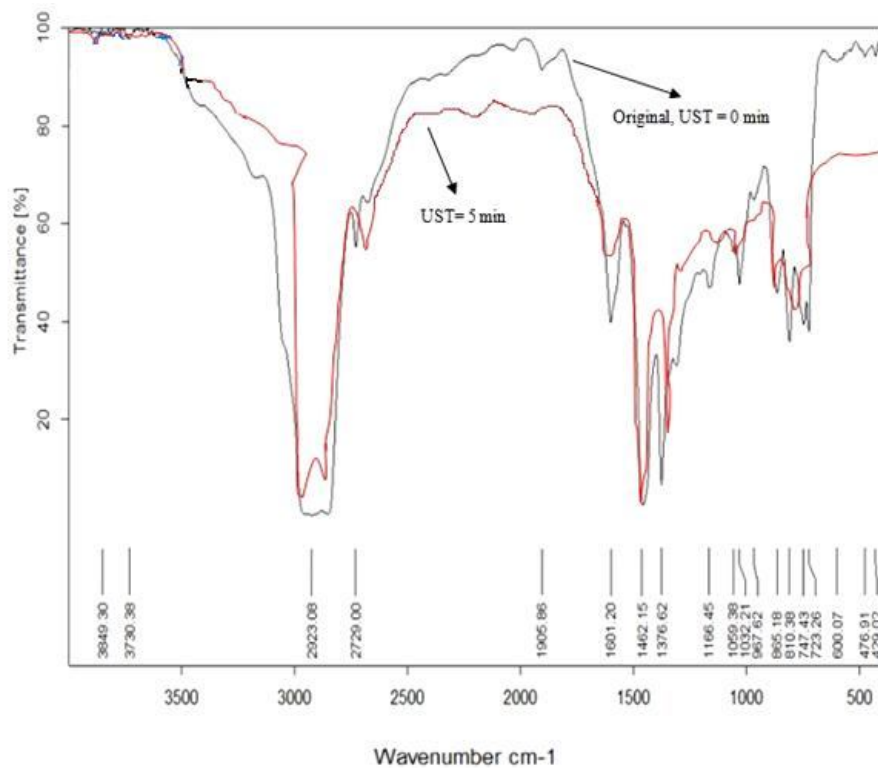


**Fig. 7.** FT-IR spectroscopy of original and irradiated samples.

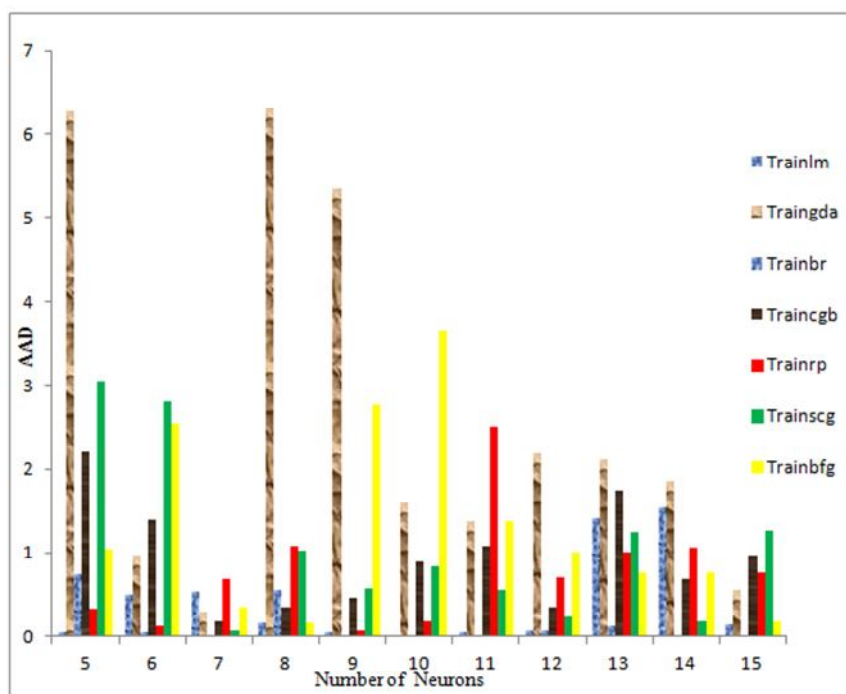


**Fig. 8.** The optimization of algorithm and neurons.

**Table 3.** The Best AAD Values of Different Training Algorithms of ANN Model with 3-7-1 Architecture

Training algorithm	AAD
Trainlm	0.53140
Traingda	0.29960
Trainbr	0.01070
Traincgb	0.18000
Trainrp	0.69030
Trainscg	0.07035
Trainbfg	0.36050

**Table 4.** The ANN Training Parameters

Parameters	Value
Network type	Feed-forward back propagation
Algorithm	Bayesian regulation
Number of input nodes	3.0000
Number of hidden neurons	7.0000
Number of output node	1.0000
Number of epochs	33.0000
Error goal	0.0001
Mu	0.0500

input data in the ANN model. Therefore, the number of input and output neurons was determined 3 and 1, respectively. There are no theoretical methods for measuring the proper number of hidden layers and their neurons. Therefore, the trail-and-error method is employed to the optimum architecture of the ANN model.

To this end, MATLAB software has several algorithms employed with different structures and many runs. Various hidden layers and the number of neurons were continuously examined. Moreover, to obtain suitable weights and biases,

runs were frequently repeated. Figure 8 depicts algorithms and number of neurons for determination of optimum algorithm and neurons. As shown in this figure, great performance was attained by seven neurons in one hidden layer. The figure depicts the Bayesian Regulation (BR) algorithm with minimum of AAD is the best. Table 3 shows the absolute average deviation (AAD) for each algorithm.

Therefore, the ANN structure of 3-7-1 was selected as optimum topology. This configuration can be seen in Fig. 9. An increase in the number of hidden neurons may lead to

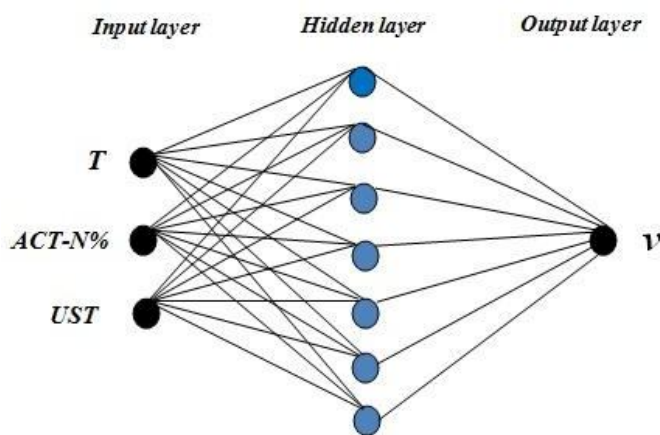


**Fig. 9.** The configuration of the ANN model.

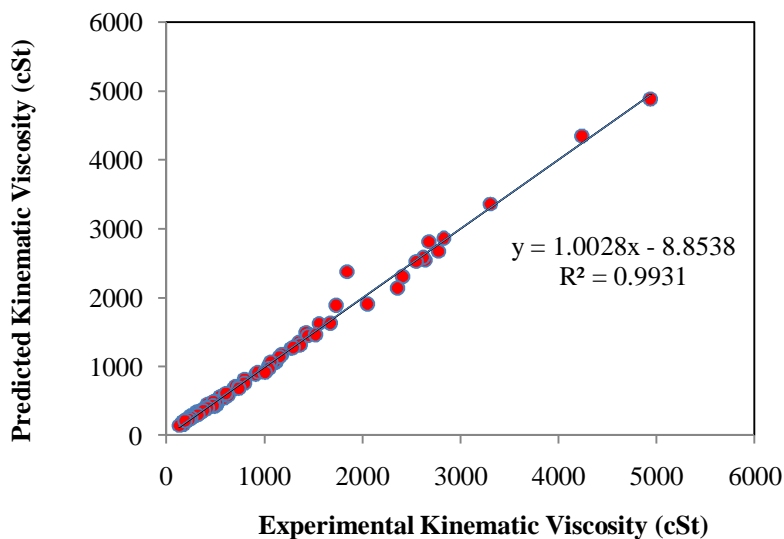


**Fig. 10.** Comparison between experimental and predicted kinematic viscosity of ANN model.

complex calculations and consuming of much time without major effect on the results and target data.

In this present study, the ANN structure of 3-7-1, feed-forward back propagation type and Bayesian Regulation (BR) algorithm were used because of their superior performance. The training parameters are reported in Table 4.

The ANN model is capable and powerful tool for estimation of kinematic viscosity of fuel oil with successful results. Figure 10 demonstrates a comparison between the

experimental data and predicted output of the ANN model. This figure reveals that the ANN predicted data approaches adaptability to the experimental data. This confirms high accuracy of the proposed ANN model.

In this research, the developed ANN model with three layers and 3-7-1 configuration supplied the appropriate weights and biases which are presented in Table 5. The kinematic viscosity was calculated based on these weights and biases. After selection of suitable weights and biases due to the number of layers and neurons of each layer, the

**Table 5.** The Best Connection Weights and Biases

Neuron	w <sub>1</sub>			b <sub>1</sub>	b <sub>2</sub> = 16.6319
	T	ACT-N%	UST		
1	14.1381	0.830980	-11.74860	-9.76350	1.7935
2	-9.0322	0.050116	9.70260	1.27190	-17.8482
3	-9.5897	4.489200	11.15830	0.23675	18.1569
4	-10.4023	2.083500	19.43240	1.21750	17.2428
5	-4.7473	-0.382980	3.85970	-0.07672	30.1495
6	2.8642	-1.939300	-7.98980	6.86330	26.9260
7	3.6956	3.685500	-0.65557	3.37050	12.6202

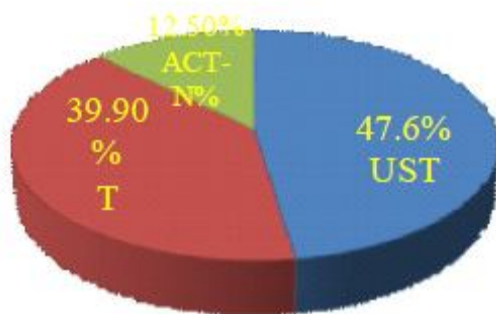


**Fig. 11.** Relative importance of input variables to prediction of kinematic viscosity.

arithmetic expression passes from the related transfer functions in the hidden and output layers according to the following equation:

$$v = F_{to} \left\{ \sum_{j=1}^7 w_{kj} \left[ F_{th} \left( \sum_{i=1}^3 w_{ji} X_i + b_j \right) \right] + b_k \right\} \quad (15)$$

where w is the weight, X is the input variable, b is the bias, i, j and k refer to the input, hidden and output layers. F<sub>th</sub> and F<sub>to</sub> are the transfer functions of hidden and output layers, respectively.

F<sub>th</sub> and F<sub>to</sub> as two effective functions are very important in the normalization and convergence of data points. In this study, the "tansig" and "purelin" were employed as transfer

functions of hidden and output layers.

Finally, in order to find the effect of input variables on the ANN predicted output, importance degree of variables was determined. The relative importance of each input variable was determined based on their weights. Figure 11 indicates the relative importance of temperature, acetonitrile concentration and ultrasonic irradiation time. As shown in this figure, the ultrasonic irradiation time has maximum of relative importance and minimum relative importance is related to acetonitrile concentration in the viscosity reduction of ANN model.

Besides all of above works, the ANN model, as a general model for the estimate of kinematic viscosity, prevents in direct the curve fitting of a large number of equations such as exponential, linear, logarithmic, power

and so on. Therefore, it can be useful in terms of time and cost. Therefore, the ANN model as a multilayer network including many equations is able to take the input variables and find the kinematic viscosity of fuel oil with a good accuracy. Using correct data of kinematic viscosity can give better results in research and development of different industries, petroleum industry specially.

### The ANFIS Modeling

In another part of this research, in order to compare the ANN model and more investigation of experimental data, the ANFIS model was also developed. First, loading train and test data were carried out in the ANFIS environment of the MATLAB software. Then, grid partition and subtractive clustering algorithms were evaluated at the fuzzy inference system (FIS) generation part. Moreover, optimization method should be determined in training section. Two optimization methods, namely, hybrid and back propagation with their epoch number (EN) were employed in the training of data. The grid partition revealed that FIS generation network was complex with high errors compared with the subtractive clustering method, because of the generation of excess number of rules. Results showed that the subtractive clustering technique and hybrid optimization method were in good agreement with experimental data. These methods were powerful in capturing the optimum relationships with lower errors than other methods. In the first step, training process of subtractive clustering method was employed by changing epoch number (EN) at default values, range of influence (ROI) = 0.5, squash factor (SF) = 1.25, accept ratio (AR) = 0.5 and reject ratio (RR) = 0.15. Results depicted that the training process achieved to the lowest error, at the epoch number of 20 for all default parameters. An absolute average deviation (AAD) of 0.0413 was obtained for default clustering parameters. In the second step, the clustering parameters were manipulatively varied until the best points were determined based on the lowest AAD value. In this method, three parameters were held at constant at their default and the fourth value was changed. The ranges of the subtractive clustering parameters (ROI = 0.1-0.6, SF = 1.2-1.35, AR = 0.1-0.3 and RR = 0.1-0.2) were evaluated based on the performance index of AAD. Results depicted the following values for the optimum parameters; ROI = 0.42, SF = 1.27, AR = 0.21 and

RR = 0.12. Minimum testing the AAD value was measured at 0.0371 by applying the optimum parameters and epoch number of 20. The testing the AAD values for the ranges of the subtractive clustering parameters is illustrated in Fig. 12. In the last step, the optimum parameters of previous step (ROI = 0.42, SF = 1.27, AR = 0.21 and RR = 0.12) were more optimized by altering the epoch number (EN) in the range of 1-100. As shown in Fig. 13, epoch numbers from 1 to 26 had some minimum and maximum of AAD and after of 26 were constant. Finally, optimized epoch number of 26 was obtained with the lowest AAD value of 0.03591, as the best prediction of kinematic viscosity of RFO.

The number of nonlinear parameters, the number of linear parameters and the number of fuzzy rules were calculated as 36, 24 and 6, respectively. Finally, the optimum ANFIS configuration (ROI = 0.42, SF = 1.27, AR = 0.21, RR = 0.12 and EN = 26) for estimation of kinematic viscosity of RFO is demonstrated in Fig. 14.

The Gaussian membership function was used as an appropriate and simple membership function. In the present work, input variables according to Table 2 (336 data points) were fuzzified with six Gaussian membership functions, labeled as MF1-MF6. The parameters of these membership functions are listed in Table 6. The rules based on the first-order sugeno inference system present the physical property of the model due to membership functions which are given in Table 7. The rules were measured based on the optimum conditions. In addition, output variable is the linear function of the input variables.

Prediction validity of the predicted kinematic viscosity is shown in Fig. 15. This figure reveals a comparison between the experimental values and ANFIS predicted data. The accuracy of the ANFIS model is illustrated in this figure. The results show that the ANFIS approach is in superior agreement with the measured data. The validity of the predicted kinematic viscosity indicates verification of the proposed model.

### The Comparison between the Developed Models

The performance of the proposed ANN and ANFIS models were statistically measured by the absolute average deviation (AAD), the average relative deviation (ARD) and coefficient of correction ( $R^2$ ) for kinematic viscosity prediction of RFO. As seen in Table 8, the performance of

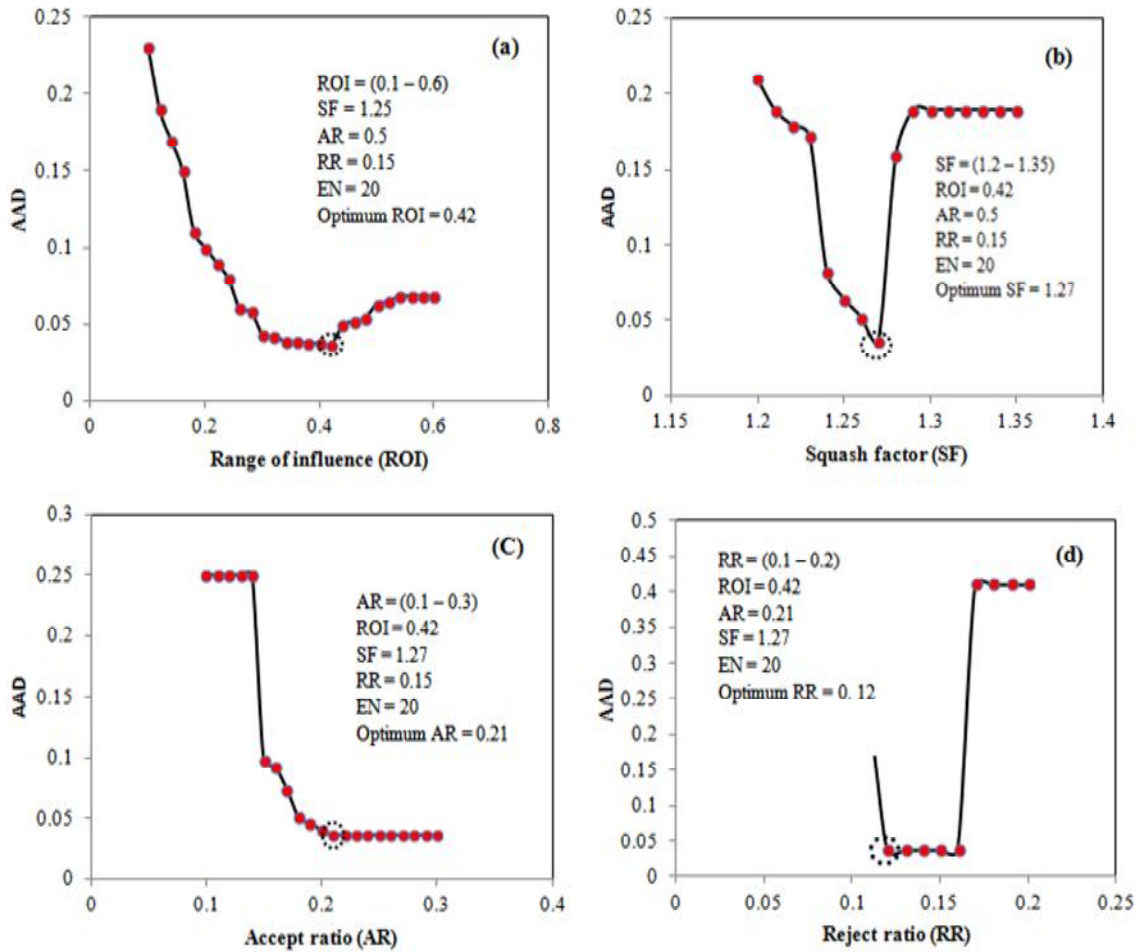


Fig. 12. Optimization of clustering parameters of the ANFIS model (Minimum testing AAD = 0.0371, EN = 20).

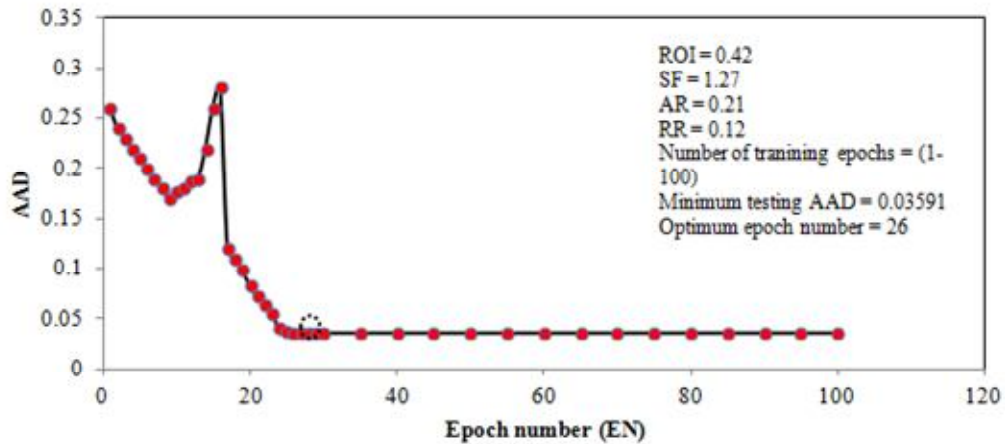
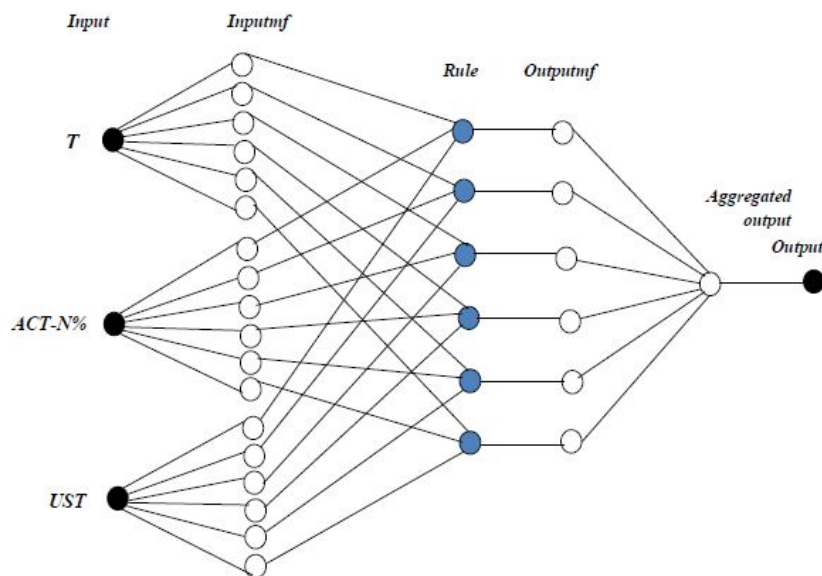


Fig. 13. Optimization of training epochs of the ANFIS model.



**Fig. 14.** The optimum ANFIS structure for prediction of kinematic viscosity of RFO (ROI = 0.42, SF = 1.27, AR = 0.21, RR = 0.12, EN = 26).

**Table 6.** Parameters of Gaussian Membership Functions for the Optimum Structure of ANFIS (ROI = 0.42, SF = 1.27, AR = 0.21, RR = 0.12, EN = 26)

$f(x, \sigma, c) = \exp\left(-\frac{1}{2}\left(\frac{x-c}{\sigma}\right)^2\right)$	Input 1, T		Input 2, ACT-N%		Input 3, UST	
	$\sigma$	$c$	$\sigma$	$c$	$\sigma$	$c$
MF1	4.5231	40.048	0.4111	0.5012	1.5260	9.9880
MF2	4.4583	39.998	0.4775	0.3018	1.4840	5.0003
MF3	4.4546	50.000	1.4926	0.3594	1.4834	4.9910
MF4	4.4543	50.100	0.8856	0.5206	1.4839	10.0003
MF5	4.4600	38.900	0.6470	3.8857	1.4848	10.1110
MF6	4.3100	40.100	0.7112	3.9731	1.5434	4.9822

$\sigma$  and  $c$  represent the variance and Gaussian MFs center, respectively.

the indicators obviously revealed that the ANN and ANFIS models estimate the target data with the lowest error in train, test and overall sets.

Results show that the ANN model leads to the lower error in forecasting the kinematic viscosity compared with

the ANFIS model. However, although the ANN model shows more precision, the ANFIS training duration is very transient. In addition, there is not vagueness in the ANFIS model compared with the ANN approach, because the ANFIS presents all of membership functions and

**Table 7.** Fuzzy Rule Base of the Optimum First-order Sugeno Type of ANFIS Structure (ROI = 0.42, SF = 1.27, AR = 0.21, RR= 0.12, EN = 26)

Rule number	Rule description
1	If (T is T MF1) and (ACT-N% is ACT-N% MF1) and (UST is UST MF1) then $v = -60.27 \times T - 141.1 \times \text{ACT-N\%} + 323.7 \times \text{UST} + 31.57$
2	If (T is T MF2) and (ACT-N% is ACT-N% MF2) and (UST is UST MF2) then $v = 16.68 \times T - 325.7 \times \text{ACT-N\%} + 14.67 \times \text{UST} + 0.9225$
3	If (T is T MF3) and (ACT-N% is ACT-N% MF3) and (UST is UST MF3) then $v = 9.24 \times T - 340.7 \times \text{ACT-N\%} + 0.04777 \times \text{UST} + 0.1867$
4	If (T is T MF4) and (ACT-N% is ACT-N% MF4) and (UST is UST MF4) then $v = -2.228 \times T - 95.25 \times \text{ACT-N\%} + 59.15 \times \text{UST} + 5.912$
5	If (T is T MF5) and (ACT-N% is ACT-N% MF5) and (UST is UST MF5) then $v = 29.94 \times T - 149.3 \times \text{ACT-N\%} - 24.7 \times \text{UST} - 2.315$
6	If (T is T MF6) and (ACT-N% is ACT-N% MF6) and (UST is UST MF6) then $v = 7.943 \times T - 27.47 \times \text{ACT-N\%} + 6.563 \times \text{UST} + 0.9839$

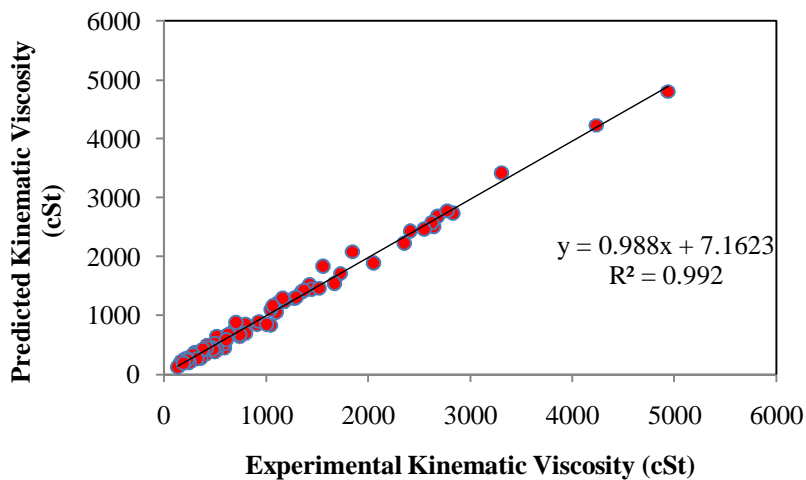


**Fig. 15.** Comparison between experimental and predicted kinematic viscosity of ANFIS model.

**Table 8.** The Performance Functions of Sets of ANN and ANFIS Model

Model	Set	Performance functions		
		AAD	ARD	R <sup>2</sup>
ANN	Training	0.00946	0.0588	0.99885
	Test	0.01110	0.0645	0.99211
	Overall	0.01070	0.0516	0.99384
ANFIS	Training	0.01237	0.0911	0.99691
	Test	0.03591	0.1086	0.99011
	Overall	0.02112	0.0992	0.99279

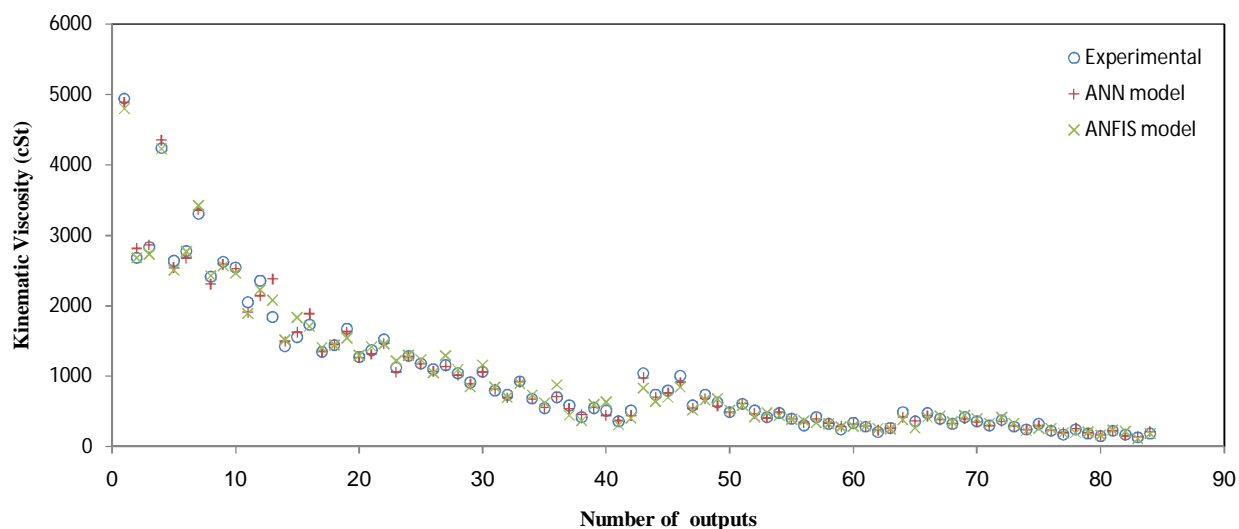


**Fig. 16.** Comparison of experimental, ANN and ANFIS models for prediction of kinematic viscosity of RFO.

relationships between inputs and predicted values. Generally, either approaches are powerful to forecast the kinematic viscosity of RFO with almost the same order of accuracy. Therefore, the ANN and ANFIS models have acceptable errors for the prediction and optimization of experimental data. Figure 16 depicts the above-mentioned facts. This figure illustrates that the models are capable of

modeling the measured data, as the ANN model has more accuracy than the ANFIS model.

## CONCLUSIONS

Kinematic viscosity as one of the important characteristics of RFO plays significant role in the

transportation and processing systems. In this work, ultrasonic irradiation and solvent were employed for decreasing the kinematic viscosity of RFO. The most important feature of this study is prediction and optimization of the experimental data by developing the artificial neural network (ANN) and adaptive neuro-fuzzy inference system (ANFIS). The ANN and ANFIS models are simple and free from defining the complex and tedious mathematical equations for prediction and optimization of viscosity. Eighty-four samples including 336 data points were trained by the ANN and ANFIS approaches. Temperature (T), solvent volumetric concentration (ACT-N%) and ultrasonic irradiation time (UST) as input variables and kinematic viscosity as output variable were considered. Results demonstrated that precision and accuracy of the predicted outputs of the ANN model were more than those of the ANFIS. Nevertheless, short duration of training and presence of clear relationships between input and output values are advantages of the ANFIS approach. However, the results illustrated that both approaches are in high accuracy and reliability for estimation the kinematic viscosity. Therefore, it can be concluded that two methods are convenient and capable in prediction and optimization of the kinematic viscosity characteristic in the high viscosity oils.

### Nomenclatures

ACT-N	Solvent volumetric concentration (vol.%)
API	American Petroleum Institute
ASTM	American Society for Testing Materials
$d^{20}$	density at 20°C (g cm <sup>-3</sup> )
RFO	residue fuel oil
T	temperature (°C)
UAE	United Arab Emirates
UST	ultrasonic irradiation time (min)
X	network input
<i>Greek letters</i>	kinematic viscosity (cSt or mm <sup>2</sup> s <sup>-1</sup> )
<i>Subscriptsi</i>	input layer
j	hidden layer
k	output layer
t	transfer function
th	transfer function of hidden layer
to	transfer function of output layer

### ACKNOWLEDGMENTS

Authors would like to thank the Research Institute of petroleum industry of Kermanshah and Kermanshah Oil Refinery for providing of samples and their valuable suggestions of advisors during this work.

### REFERENCES

- [1] Kent, J. A., Riegel's Handbook of industrial chemistry, Springer: **1983**.
- [2] Perry, R. H.; Green, D. W., Perry's Chemical Engineers Handbook, McGraw-Hill: **1997**.
- [3] Gray, M. R., Upgrading of Petroleum Residue and Heavy Oil, CRC Press: **1994**.
- [4] David, S. J.; Pujado, P. R., Handbook of Petroleum Processing, Springer: **2006**.
- [5] Heinemann, H.; Spelght, J. G., The Chemistry and Technology of Petroleum, Taylor and Frances Group: **2006**.
- [6] Simanzhenkov, V.; Idem, R., Crude Oil Chemistry, Marcel Dekker: **2003**.
- [7] Allen, T. D.; Roberts, A. P., Production Operations: Well Completion, Workover and Stimulation, Oil & Gas Consultants International: **1982**.
- [8] Hirscherg, A.; Dejong, N. J.; Schipper, B. H.; Meijer, J. G., Influence of Temperature and Pressure on Asphaltene Flocculation, Society of Petroleum Engineering of AIME: **1984**.
- [9] Gunal, O. G.; Islam, M. R., Alteration of asphaltic crude oil rheology with electromagnetic and ultrasonic irradiation, *J. Petroleum Sci. Eng.*, **2000**, 26, 263-272, DOI: 10.1016/S0920-4105(00)00040-1.
- [10] Timothy, J. M.; John, P. L., Applied Sonochemistry: Uses the Power Ultrasound in Chemistry and Processing, Wiley-VCH Verlag GmbH & Co. KGaA: **2002**.
- [11] David, J.; Cheeke, N., Fundamentals and Applications of Ultrasonic Waves, CRC Press: **2002**.
- [12] Shedid, S. A., An ultrasonic irradiation technique for treatment of asphaltene deposition, *J. Petroleum. Sci. Eng.*, **2004**, 42, 57-70, DOI: 10.1016/j.petrol.2003.11.001.
- [13] Gogate, P. R., Cavitation reactors for process

- intensification of chemical processing applications: A critical review, *Chem. Eng. Process. Process Intensif.*, **2008**, *47*, 515- 527, DOI: 10.1016/j.cep.2007.09.014.
- [14] Hongfu, F.; Yongjian, L.; Liying, Z.; Xiaofei, Z., The study on composition changes of heavy oils during steam stimulation processes, *Fuel*, **2002**, *81*, 1733-1738, DOI: 10.1016/S0016-2361(02)00100-X.
- [15] Bjorndalen, N.; Islam M. R., The effect of microwave and ultrasonic irradiation on crude oil during production with a horizontal well, *J. Petroleum. Sci. Eng.*, **2004**, *43*, 139-150, DOI: 10.1016/j.petrol.2004.01.006.
- [16] Hong-Xing, X.; Chun-Sheng, P., Experimental study of heavy oil underground aquathermolysis using catalyst and ultrasonic, *J. Fuel Chem. Technol.*, **2011**, *39*, 606-610, DOI: 10.1016/S1872-5813(11)60037-6.
- [17] Wang, R.; Liu, J.; Hu, Y.; Zhou, J.; Cen, K., Ultrasonic sludge disintegration for improving the co-slurrying properties of municipal waste sludge and coal, *Fuel Process. Technol.*, **2014**, *125*, 94-105, DOI: 10.1016/j.fuproc.2014.03.014.
- [18] Saikia, B. K.; Dutta, A. M.; Saikia, L.; Ahmed, S.; Baruah, B. P., Ultrasonic assisted cleaning of high sulphur Indian coals in water and mixed alkali, *Fuel Process. Technol.*, **2014**, *123*, 107-113, DOI: 10.1016/j.fuproc.2014.01.037.
- [19] Jialei, H.; Xingang, L.; Hong, S., The optimization and prediction of properties for crude oil blending, *Comput. Chem. Eng.*, **2015**, *76*, 21-26, DOI: 10.1016/j.compchemeng.2015.02.006.
- [20] Karuppiyah, R.; Furman, K. C.; Grossmann, I. E., Global optimization for scheduling refinery crude oil operations, *Comput. Chem. Eng.*, **2008**, *32*, 2745-2766, DOI: 10.1016/j.compchemeng.2007.11.008.
- [21] Oddsdottir, T. A.; Grunow, M.; Akkerman, R., Procurement planning in oil refining industries considering blending operations, *Comput. Chem. Eng.*, **2013**, *58*, 1-13, DOI: 10.1016/j.compchemeng.2013.05.006.
- [22] Chen, X.; Grossmann, I.; Zheng, L., A comparative study of continuous-time models for scheduling of crude oil operations in inland refineries, *Comput. Chem. Eng.*, **2012**, *44*, 141-167, DOI: 10.1016/j.compchemeng.2012.05.009.
- [23] Yetilmezsoy, K.; Fingasb, M.; Fieldhouse, B., An adaptive neuro-fuzzy approach for modeling of water-in-oil emulsion formation, *Colloids Surf. A: Physicochem. Eng. Aspects*, **2011**, *389*, 50-62, DOI: 10.1016/j.colsurfa.2011.08.051.
- [24] Dasila, P. K.; Choudhury, I. R.; Saraf, D. N.; Kagdiyal, V.; Rajagopal, S.; Chopra, S. J., Estimation of FCC feed composition from routinely measured lab properties through ANN model, *Fuel Process. Technol.*, **2014**, *125*, 155-162, DOI: 10.1016/j.fuproc.2014.03.021.
- [25] Vasseghian, Y.; Heidari, N.; Ahmadi, M.; Zahedi, G.; Mohsenipour, A. A., Simultaneous ash and sulfur removal from bitumen: Experiments and neural network modeling, *Fuel Process. Technol.*, **2014**, *125*, 79-85, DOI: 10.1016/j.fuproc.2014.03.023.
- [26] Tay, J. H.; Zhang, X., A fast predicting neural fuzzy model for high-rate anaerobic waste water treatment systems, *Water Res.*, **2000**, *34*, 2849-2860, DOI: 10.1016/S0043-1354(00)00057-9.
- [27] Altunkaynak, A.; Ozger, M.; Cakmakci, M., Fuzzy logic modeling of the dissolved oxygen fluctuations in Golden Horn, *Ecologic. Model.*, **2005**, *189*, 436-446, DOI: 10.1016/j.ecolmodel.2005.03.007.
- [28] Cakmakci, M., Adaptive neuro-fuzzy modeling of anaerobic digestion of primary sedimentation sludge, *Bioproc. Biosyst. Eng.*, **2007**, *30*, 349-357, DOI: 10.1007/s00449-007-0131-2.
- [29] Olatunji, S.O.; Selamet, A.; Abdul, R. A. A., Predicting correlations properties of crude oil systems using type-2 fuzzy logic systems, *Expert Syst. Appl.*, **2011**, *38*, 10911-10922, DOI: 10.1016/j.eswa.2011.02.132.
- [30] Standard Test Method for Kinematic Viscosity of Transparent and Opaque Liquids (and Calculation of Dynamic Viscosity), **2012**.
- [31] Standard Test Method for Density, Relative Density, or API Gravity of Crude Petroleum and Liquid Petroleum Products by Hydrometer Method, **2012**.
- [32] Standard Test Method for Pour Point of Petroleum Products, **2012**.
- [33] Standard Test Method for Ash from Petroleum Products, **2012**.
- [34] Standard Test Method for Flash and Fire Points by

- Cleveland Open Cup Tester, **2012**.
- [35] Demuth, H.; Beale, M., Neural network toolbox for use with MATLAB. The MathWorks: **2000**.
- [36] Jang, J. S. R., ANFIS-Adaptive-network-based fuzzy inference system, *IEEE Trans. Syst. Man Cybern.*, **1993**, *23*, 665-685, DOI: 10.1109/21.256541.
- [37] Atmaca, H.; Cetisli, B.; Yavuz, H. S., The comparison of fuzzy inference systems and neural network approaches with ANFIS method for fuel consumption data, in: Second International Conference on Electrical and Electronics Engineering Papers ELECO'2001, Bursa, Turkey, **2001**.
- [38] Tsukamoto, Y., An approach to fuzzy fuzzy reasoning method, *Advances in fuzzy set theory and applications*, North-Holland, Amsterdam: **1979**.
- [39] Takagi, T.; Sugeno, M., Fuzzy identification of systems and its applications to modeling and Control, *IEEE Trans. Syst. Man. Cybern.*, **1985**, *15*, 116-132, DOI: 10.1109/TSMC.1985.6313399.
- [40] Cakmakci, M.; Kinaci, C.; Bayramoglu, M.; Yildirim, Y., A modeling approach for iron concentration in sand filtration effluent using adaptive neuro-fuzzy mode, *Expert Syst. Appl.*, **2010**, *37*, 1369-1373, DOI: 10.1016/j.eswa.2009.06.082.
- [41] Chiu, S., Fuzzy model identification based on cluster estimation, *J. Intell. Fuzzy Syst.*, **1994**, *2*, 267-278, DOI: 10.3233/IFS-1994-2306.
- [42] Yager, R.; Filev, D., Generation of fuzzy rules by mountain clustering, *J. Intell. Fuzzy Syst.*, **1994**, *2*, 209-219, DOI: 10.3233/IFS-1994-2301.
- [43] Leontartits, K. J.; Mansoori, G. A., Asphaltene Deposition: A survey of field experiences and research approaches, *J. Petroleum Sci. Eng.*, **1988**, *1*, 229-239, DOI: 10.1016/0920-4105(88)90013-7.
- [44] Fuse, T.; Hirota, Y.; Kobayashi, N.; Hasatani, M.; Tanaka, Y., Characteristics of low vapor pressure oil ignition developed with irradiation of mega hertz level ultrasonic, *Fuel*, **2004**, *83*, 2205-2215, DOI: 10.1016/j.fuel.2004.06.001.
- [45] Ernest, L. R.; James, J.; Moran, D. T.; Robert, D. T., Measurement Problems in the Instrument and Laboratory Apparatus Fields, in *Systems of Units, National and International Aspects*, American association for the advancement of science: **1959**.